Title
ANGLE- AND ENERGY-DEPENDENT CORE-LEVEL PHOTOELECTRON ENERGY LOSS STUDIES IN Al AND In

Author
Williams, R.S.

Publication Date
1977

Submitted to Journal of Electron
Spectroscopy and Related Phenomena

LBL-6027
Preprint

ANGLE- AND ENERGY-DEPENDENT CORE-LEVEL PHOTOELECTRON ENERGY LOSS STUDIES IN Al AND In

R. S. Williams, S. P. Kowalczyk, P. S. Wehner,
G. Apai, J. Stöhr, and D. A. Shirley

January 1977

Prepared for the U. S. Energy Research and
Development Administration under Contract W-7405-ENG-48

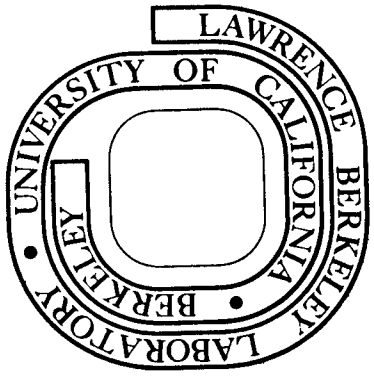

DISCLAIMER

ANGLE- AND ENERGY-DEPENDENT CORE-LEVEL PHOTOELECTRON ENERGY LOSS STUDIES IN Al and In*

R. S. Williams, S. P. Kowalczyk,+ P. S. Wehner,

G. Apai, J. Stöhr, and D. A. Shirley

Materials and Molecular Research Division
Lawrence Berkeley Laboratory
and
Department of Chemistry
University of California
Berkeley, California 94720

ABSTRACT

Electron energy loss structures of Al and In core-level photoemission spectra, in particular surface and bulk plasmon losses, have been investigated as functions of photon energy (i.e., photoelectron kinetic energy). These studies utilized synchrotron radiation to provide a variable photon source in the ultra-soft x-ray region, thus allowing these loss processes to be studied at photoelectron kinetic energies for which the mean free path of the electrons is at a minimum. The Al plasmon loss structure was also studied with soft x-ray radiation in an angle-resolved mode, allowing the variation of effective photoelectron sampling depth with different electron take-off (collection) angles. These results for the relative intensity of the bulk and surface plasmons as a function of electron kinetic energy and electron exit angle are in qualitative agreement with the predictions of Šunjić and Šokčević. The core-level binding energies of surface atoms have also been studied with the result that no significant shift has been observed with respect to bulk-atom core levels.

I. INTRODUCTION

In the past several years photoemission spectroscopy (PES) has become a widely used probe of the electronic structure of solids, with increasing emphasis being placed on the surface capabilities of this and other low-energy electron spectroscopies.[1-4] Our understanding of photoemission is still developing.[5,6] For heuristic purposes, the photoemission process in solids may be explained in terms of the three-step model discussed by Berglund and Spicer.[7] Within the framework of this model, the first step (electron photoexcitation) is responsible for the observed peaks in a photoelectron spectrum. The other two steps (transport through the solid and escape into vacua) contribute the background of electrons scattered out of the main peaks. However, these background effects, such as electron-hole coupling, plasmon excitations, collisionally induced inter-band transitions, etc.[8,9] contribute structure to the photoelectron spectrum which may, as in the case of free-electron-like metals,[10] contain more spectral intensity than the main photoemission peaks.

The study of this background structure, especially plasmon loss peaks, yields important information about the electronic structure of solids.[11] Surface and bulk plasmon frequencies are easily determined via PES. Recent studies of plasmon satellites have relied on intensity analysis to determine the importance of intrinsic versus extrinsic processes in plasmon excitation.[12-15] This paper is concerned mainly with the relation of experimentally observed plasmon loss intensities to the inelastic mean free path (Λ_{ee}) of photoelectrons propagating through a sample.

In this work, surface and bulk plasmon loss intensities normalized to the main peak intensity were studied in the PES spectra of Al and In. The variations of these relative intensities were studied as functions of electron take-off (for Al only) and electron kinetic energy E_o (which we were able to vary due to the availability of a synchrotron radiation source). These two parameters determine the effective sampling depth for the photoelectrons which escape into the vacuum. During the course of these studies, we also attempted to detect possible binding energy differences between bulk and surface atoms; however, no binding energy shifts were observed. Section II presents the experimental details of this investigation. The results for Al and In bulk and surface plasmon intensities are reported in Section III and are compared with theoretical predictions in Section IV.

II. EXPERIMENTAL

The photoemission measurements reported in this paper were performed in two separate experimental chambers. The measurements involving electron take-off angle were conducted in a specially modified Hewlett-Packard Model HP 5950A electron spectrometer[16] which utilizes a monochromatized Al Kα ($\hbar\omega$ = 1486.6 eV) radiation source. The dispersion compensation lens system has an electron angular acceptance cone of approximately 15 msterad,[17] which is sufficiently narrow for our angle-resolved studies. The details of the angle variation procedure have been previously reported.[18] The measurements dealing with plasmon intensity variations due to changes in initial electron kinetic energy were performed in an ion-pumped UHV stainless steel bell jar system installed on the 4° station of Beam Line I at the Stanford Synchrotron

Radiation Project (SSRP).[19] The photon source was synchrotron radiation from the electron-positron storage ring SPEAR at the Stanford Linear Accelerator Center (SLAC). The radiation was monochromatized and the photon energy was varied by a grazing incidence "grasshopper" monochromator.[20] Photoelectrons were energy analyzed with a double-pass cylindrical mirror analyzer. (CMA), Physical Electronics Model PHI 150255G. The experimental geometry is shown in Fig. 1. Note that the experimental geometry was chosen to integrate over electron take-off angles between normal and grazing escape.

A freshly evaporated aluminum film was used in the angle variation studies. Possible carbon and oxygen contaminants were monitored by scanning the photoemission spectral regions near their respective 1s binding energies. Contaminant levels were below the detection sensitivity of XPS, i.e. less than 0.1 monolayer. The Al sample used for the synchrotron radiation studies was an evaporated film from a 99.999% pure foil on a stainless steel substrate. Repeated depositions of Al were required to minimize the intensity of the oxide satellite of the Al 2p peak. The base pressure of the system was $\leq 2 \times 10^{-10}$ torr and the relative intensities of the Al 2p and its oxide satellite did not change during the 26 hour duration of the experiment. The In sample was cut from an ingot of 99.999% pure In. The sample was mechanically polished, then etched in warm aqua regia immediately prior to installation in the experimental chamber. The base pressure in the chamber was 1×10^{-9} torr, as no bakeout was performed. The sample was Ar^+ ion-bombarded briefly to remove surface impurities. The In spectra revealed no core line shifts due to contamination.

In order to analyze the relative intensities of the core peaks and plasmons, the spectra were least-squares fitted to gaussian peak shapes plus a background using the program GAMET.[21] The overall spectral background and individual peak tail functions were chosen to yield a best fit to the experimental data, and do not necessarily represent a justifiable separation of physical effects (i.e electron-hole coupling) from the main peaks. However, processes causing peak asymmetries should be self cancelling when considering relative intensities.

III. RESULTS

Surface sensitivity enhancement in XPS via low electron take-off angles

1. Variation of effective electron escape depth with electron take-off angle.

In 1969 Harris[22] showed that the surface sensitivity in Auger electron emission is enhanced by using low electron take-off angles ϕ. Enhancement of surface sensitivity in XPS by this technique was first demonstrated by Fraser *et al.*[23] and by Fadley *et al.*[24] Subsequently Fadley and co-workers have carried out detailed studies of the effects of such parameters as surface roughness on the ϕ-dependence of XPS spectra.[25] In this section we present data illustrating the surface enhancement effect for the 2s line of aluminum at XPS energies.

Values of the electron attenuation length Λ_{ee} have been measured for a variety of solids by the use of such methods as overlayer deposition.[26-29] For XPS photoelectrons from loosely-bound orbitals (kinetic energies $\sim$ 1000 eV), the Λ_{ee} values lie in the 15-30 Å range. Thus in

normal emission the effective sampling depth Λ'_{ee} is 5-10 atomic layers. In Fig. 2 we illustrate the relation between Λ'_{ee} and ϕ, defined as the angle between the electron propagation direction and the sample plane. Clearly,

$$\Lambda'_{ee} = \Lambda_{ee} \sin \phi \quad . \tag{2}$$

Thus for $\Lambda_{ee} \sim$ 15-30 Å, observation at practically achievable angles ($\phi \sim 5^\circ$-10°) will give very high surface sensitivity.

Figure 3, which shows the Al 2s spectra taken at $\phi = 7.5^\circ$ and $\phi = 51.5^\circ$ from the same Al film, demonstrates this sensitivity. The Al film was freshly evaporated from an Al charge which was not completely outgassed (the measurement at $\phi = 7.5^\circ$ was obtained before that at $\phi = 51.5^\circ$). Spectrum (b) shows just one peak with an asymmetry to higher binding energy which is often seen in metals and generally attributed to electron-hole coupling.[30,31] However, spectrum (a) clearly reveals two peaks, one due to the metal and one due to a surface oxide. In the case of Fig. 3, the surface sensitivity of spectrum (b) was increased by approximately a factor of six over that in spectrum (a). Thus Λ_{ee} in XPS can become as low as 2 Å or nearly one atomic layer. Such surface sensitivity enhancement should be of great utility in investigating surface phenomena and in differentiating between surface and bulk contributions to XPS spectra. This is a practical method of depth profiling in a non-destructive manner, i.e., without having to ion-sputter.

2. Angular dependence of Al 2s surface and bulk plasmon loss relative intensities.

Figure 4 shows the Al 2s spectral region from an evaporated metal film in XPS measurements at three different takeoff angles. The spectra show only the Al 2s core-level peak and the first surface and bulk plasmon peaks. The binding energy of the Al 2s peak was measured to be 117.85 eV with respect to the Fermi level of Al. The surface and bulk plasmon energies, 10.5 eV and 15.2 eV respectively, agree with previously reported values (Ref. 12) and do not vary with take-off angle.

Inspection of Fig. 4 shows that the surface plasmon loss peak intensity increases greatly relative to both the primary peak and the bulk plasmon peak as the electron take-off angle is decreased. This is to be expected because at low ϕ the escaping photoelectron has a lower component of velocity normal to the surface and thus spends more time in the surface layer than an electron with higher ϕ. The bulk plasmon peak intensity relative to the primary peak decreases only slightly at lower ϕ. These observations will be discussed in more detail in Section IV.

3. Ultrasoft x-ray PES measurements: surface sensitivity variation as a function of photoelectron kinetic energy

The well known "universal curve", Fig. 5, illustrates the variation of electron attenuation length, or mean free path, with kinetic energy for nearly all materials for which these determinations have been made.[32] The strong dependence of Λ_{ee} on E_o suggests that PES experiments could be performed utilizing different photon energies to selectively probe the electronic structure of solid surfaces; i.e., photon energies would

be chosen such that the photoelectrons from the peak being studied would have a kinetic energy corresponding to the minimum possible Λ_{ee}. Unfortunately, there are too few discrete photon sources to carry out extensive measurements of this type (Fig. 5 shows the main laboratory sources now in use in relation to the universal curve). However, synchrotron radiation provides an intense source of continuous radiation throughout the range of interest. With proper monochromatization, it is possible to obtain spectra throughout the universal curve and in particular in the most surface-sensitive region.

We have carried out such experiments for the 130 eV $\leqslant \hbar\omega \leqslant$ 280 eV photon energy range using synchrotron radiation to study the Al 2p peak and with 80 eV $\leqslant \hbar\omega \leqslant$ 180 eV for the In 4d peak. These experiments were performed in an angle-integrated mode; i.e., utilizing the full acceptance cone of the CMA, due to the low count rates in the plasmon loss peaks. The spectra for the Al 2p region including the bulk (B) and surface (S) plasmons are given in Fig. 6 for several photon energies near the minimum of the universal curve. As can be seen in these spectra, the film is somewhat oxidized. For comparison, the Al 2p spectrum obtained at XPS energies is given in Fig. 7. The surface and bulk plasmon energies were independent of photoelectron kinetic energy. Representative spectra from the In 4d region are shown in Fig. 8. We determined a value of 3.46 ± 0.24 eV for the work function of In. The surface and bulk plasmon energies (8.6 and 11.7 eV respectively) displayed no measurable dispersion. The In 4d XPS spectrum (after Ref. 12) is shown in Fig. 9 for comparison.

4. Binding energies of bulk atoms vs. surface atoms

Before discussing the plasmon intensity variations, we mention some ancillary results obtained during and in conjunction with the plasmon studies. One question of importance in surface electronic structure is whether or not the core-level binding energy of a surface atom is different from the core-level binding energy of a bulk atom. The surface sensitivities achievable by our techniques should illuminate this point.

Differences between bulk- and surface-atom binding energies have been postulated on the basis of some appearance potential spectroscopy (APS) measurements on Ti, Cr, and Ni.[33] These APS measurements suggested a difference of approximately one eV and that the surface atoms had the lower binding energies. Later APS measurements by Webb and Williams[34] disputed this observation. Such a large binding energy difference should be easily observed in surface sensitive PES measurements. We have conducted a variety of experiments in an attempt to observe surface atom binding energy shifts.

Several XPS spectra were taken of core-levels of Al and Ni films which were freshly evaporated in situ under UHV conditions. These films exhibited no sign of contamination as revealed by in situ chemical analysis of core-level spectra of possible common contaminants. The measurements at low ($\phi = 7.5^{\circ}$) and high ($\phi = 51.5^{\circ}$) take-off angles found no evidence for a difference between surface and bulk binding energies, referenced to the Fermi level, within ± 0.15 eV. The low angle spectrum of Al (Fig. 4), did reveal a shoulder due to a minute amount of surface oxide (<.05 monolayer).

In our synchrotron radiation studies, the binding energies of the In 4d peaks with respect to the In Fermi level showed no discernible photon energy dependence. Also, there were no observable satellites attributable to surface atoms in the high resolution spectra taken of the In 4d levels at surface sensitive electron energies. Further evidence against large binding energy shifts of surface atoms came in angle-resolved[35] studies of the 4f levels of a clean platinum (111) single crystal surface. These studies utilized different photon energies and electron take-off angles to vary the effective photoelectron sampling depth. As in the other experiments, there were no observable satellites or binding energy shifts in the most surface sensitive PES spectra. The lack of a core level binding-energy shift between surface and bulk atoms is surprising if one attempts to understand the condensed-phase core-level binding energies in terms of free-atom values. There are large shifts (5-10 eV) from free atom values for condensed-phase binding energies.[36] These shifts are usually explained as arising from combinations of differences in initial-state charge distribution and extra-atomic relaxation. Apparently these initial and final state effects are either very small or cancel each other to a large extent. Further theoretical developments and experimental results are required to determine the nature of such electronic structure and perhaps isolate cases in which significant binding energy shifts due to atomic location exist.

IV. DISCUSSION

1. Angular dependence of Al plasmon loss intensities

A general review of plasmon excitations in solids was given by Raether.[37] Comprehensive theoretical treatments of the relation between electron mean free paths (MFP's) and plasmon satellite intensities

were given by Feibelman[9] and Šunjić and Šokčević.[11] The latter authors have treated the specific example of plasmon loss structure from the Al 2p level. We shall rely heavily on Ref. 11 as a basis for the interpretation of our data.

If we assume that the bulk plasmon excitation process is predominantly extrinsic and has the form (Ref. 13)

$$I_B^o \propto \lambda_B/(1 + \lambda_B/\Lambda_{ee})^2 \qquad (2)$$

where I_B^o is the first bulk plasmon loss to main peak intensity ratio, λ_B is the electron MFP for bulk plasmon creation events, and Λ_{ee} is the MFP for all collision processes, we see that I_B^o is independent of ϕ . A further simple assumption, that surface plasmon excitation probability is proportional to the amount of time required for a photoelectron to traverse the surface layer, yields a surface plasmon to main peak ratio (I_S^o) proportional to $(\sin \phi)^{-1}$. However, Refs. 9 and 11 have shown that the introduction of a solid-vacuum interface alters the local character of bulk (and surface) plasmon excitations. Thus surface and bulk excitation probabilities (Q_S and Q_B) become functions of the electron excitation depth (L) and takeoff angle (ϕ) as well as electron kinetic energy.

Figure 10 shows I_B^o and I_S^o as functions of Λ_{sr} and ϕ for photoelectrons excited from the Al 2p level with Mg Kα radiation (electron kinetic energy $\approx$ 1176 eV) where Λ_{sr} is the MFP due only to short-range interactions (i.e. electron-hole creation). The values for I_B^o and I_S^o were generated by fitting plasmon excitation probabilities Q_B and Q_S of

Fig. 5 in Ref. 11 to a series of line segments and performing the integration of Eq. 21 in Ref. 11 analytically. Since Šunjić and Šokčević presented plasmon excitation probabilities for only three exit angles (ϕ = 90°, 50°, and 20°), we used interpolated and extrapolated Q_B and Q_S values to compute the plasmon intensity angular dependence from normal to grazing ϕ. Thus Fig. 10 is presented only to indicate trends.

Our experimental data, presented in Table 1, represent mainly plasmon loss structure following the Al 2s peak using Al Kα radiation as an excitation source (kinetic energy = 1368 eV). However, we are still justified in comparing our experimental data to Fig. 10 since Fig. 6 and 7 in Ref. 11 show that Q_B and Q_S for Al are insensitive to 200 eV differences in electron kinetic energy above 1 keV. Baird and Fadley[38] have measured I_B^o and I_S^o at 10° intervals from grazing to normal takeoff angles for Al 2p loss features using Al Kα radiation. In general, the values we measure for plasmon loss intensities are greater than theirs; especially for I_S^o at ϕ = 38° and 54° which are over a factor of two greater in our measurements. From Table 1 and Ref. 11 it is doubtful this discrepancy is due to the difference in photoelectron kinetic energies. A possible explanation is that the Al sample used in Ref. 38 had a slight surface contamination or roughness which decreased the surface plasmon loss intensity.

Direct comparison of our experimental results to Fig. 10 indicate that the plasmon loss probabilities Q_B and Q_S have been underestimated in Ref. 11. However, the ratio I_B^o/I_S^o (which is more sensitive to Λ_{ee} and ϕ than either I_B^o or I_S^o) may still be correctly predicted. Figure 11

(I_B^o/I_S^o versus ϕ) was generated from our complete set of I_B^o and I_S^o curves taking Λ_{sr} to be 25 Å.[39] Except for small angles, the resulting I_B^o/I_S^o curve follows the sin ϕ prediction of the simple approximations mentioned at the beginning of this section. We also see surprisingly good agreement between the three experimental values and the predicted I_B^o/I_S^o ratios.

The main point of disagreement between the predictions of Fig. 10 and our experimental results is that the observed I_B^o ratio decreases with decreasing ϕ. That our computations predict the opposite behavior is most likely due to our parameterization and extrapolation of the results of Ref. 11. Since the sin ϕ behavior of I_B^o/I_S^o is valid over a large angular range, the variation of bulk plasmon excitations from a local process occurs only in a region very near the surface. For XPS spectra with a large effective sampling depth, the observed electron loss spectra can be interpreted mainly in terms of a MFP due to local bulk plasmon excitations and short-range excitations. From the slope of I_B^o ($\phi = 90^\circ$) for large Λ_{sr} one can approximate $\lambda_B = 42$ Å (λ_B is the mean free path for bulk plasmon excitation). Thus, $\Lambda_{ee} \simeq (\Lambda_{sr}^{-1} + \lambda_B^{-1})$ or 15.7 Å, which is close to the experimentally observed value of 18 Å from Ref. 24.

2. Kinetic Energy Dependence of I_B^o and I_S^o for Al and In

The variations with electron kinetic energy of I_B^o and I_S^o are shown in Fig. 12 for the Al 2p case and in Fig.13 for In 4d. All spectra were angle-integrated. A detailed interpretation is not feasible because no calculations are available which treat the explicit angle, energy, and Λ_{ee} dependence of I_B^o and I_S^o in the energy range of our experiments.

Despite repeated efforts, we were unable to produce an oxygen-free aluminum sample in the chamber we used at SSRP; an Al 2p oxide satellite peak appeared in all our spectra with ~ 30% the intensity of the main peak. However our Al plasmon intensities agree well with the spectra of S. A. Flodstrom, et al.[40] taken on an oxide-free sample at fewer energies (see Fig. 12). The Al LMM Auger peak (evident at ~ 100 eV "binding energy" in the 170 eV photon energy spectrum of Fig. 6) renders an accurate determination of I_B^o and I_S^o impractical for photon energies 130 eV < $\hbar\omega$ < 170 eV. Also, for $\hbar\omega$ < 130 eV both a strongly nonlinear inelastic electron background and rapidly decreasing plasmon intensities preclude accurate tracking of I_B^o and I_S^o to their respective threshold energies.

Figure 12 shows that for electron kinetic energies above 93 eV, I_B^o increases with energy while I_S^o decreases. The calculations of Ref. 11, which were all for initial electron kinetic energies $\geqslant$ 100 eV, showed that the bulk plasmon excitation probability decreases with increasing electron kinetic energy. This is consistent with our results if Λ_{ee} increases faster with kinetic energy than the bulk plasmon excitation probability decreases. Figure 7 in Ref. 11 also shows that the surface plasmon excitation probability can increase or decrease rapidly in the energy range around 100 eV, depending on the effective escape depth sampled. The observed slight decline in intensity is most likely due to sufficiently large (~ 3Å) and steadily increasing Λ_{ee} for electron kinetic energies between 93 and 193 eV. From Ref. 39 we see that Λ_{ee} in Al is predicted to be a minimum (~ 3Å) at 50 eV and rise to 6Å at 200 eV, which is in qualitative agreement with Fig. 5 (the calculations

of Kleinman[41] place the minimun of Λ_{ee} near 15 eV and are thus not in accord with experimental observations). At these low electron kinetic energies much of the plasmon loss signal originates in a region where the bulk plasmon excitation process is non-local, thus requiring very detailed calculations to predict the angle and energy dependence of the plasmon loss peaks.

The observed I_B^o/I_S^o ratio for Al at 53 eV is greater than or equal to that in the range of 93-123 eV. By the considerations of the preceding paragraph and Fig. 10 this would indicate that the minimum in Λ_{ee} occurs somewhere between 53 eV and 93 eV kinetic energy. In this case a better determination is not possible due to the Auger interference in the region of interest. Further complications in the interpretation of plasmon intensity data may also arise due to elastic electron scattering from the surface potential considered in Ref. 29.

The predicted Λ_{ee} for In is lower than for Al at all electron kinetic energies,[42] so surface effects should be more enhanced for In over Al. Indeed, we observe, (Figs. 6-9) that the ratio I_B^o/I_S^o for In is much lower than for Al, although the bulk plasmon excitation probability is smaller for In. Figure 13 shows that I_B^o and I_S^o for In are nearly equal over the range of electron energies 53-123 eV, and change little with energy. We observe a narrow energy region over which $I_S^o > I_B^o$ ($\hbar\omega$ = 160 eV) and the intensities then invert ($\hbar\omega$ = 180 eV). The electron kinetic energy of this very surface sensitive region is around 143 eV, which is near the bottom of the universal curve. However, there may be a resonant process which accounts for the apparent narrow minimum in Λ_{ee} which has not been explored theoretically thus far.

V. CONCLUSIONS

This investigation has demonstrated that surface sensitivity in PES can be greatly enhanced by either using low electron take-off angles or by utilizing a photon energy such that the photoelectron kinetic energy is near the minimum of the "universal curve". Further, the surface sensitivity of a particular take-off angle and energy can be monitored by observing surface and bulk plasmon loss intensities. No differences have been found in core-level binding energies of surface and bulk atoms in Al, Ni, In, or Pt utilizing surface sensitive PES measurements. The angular dependence of the bulk to surface plasmon ratios was predicted quite well by Šunjić and Šokčević.[11] In principle, if a set of theoretical calculations like those illustrated in Fig. 10 were available for a complete set of angles and a series of electron energies, angle resolved PES spectra at several different take-off angles could be used to determine the Λ_{ee} versus kinetic energy curve for materials with plasmon structure. The accuracy of these determinations depends on the quality of the calculated values, which may already be as good as experimental overlayer techniques.

Acknowledgements

We would like to acknowledge the assistance of Dr. Lothar Ley and Dr. F. Read McFeely, who participated in the XPS experiments performed on the Al and Ni films. We would also like to thank Dr. Charles S. Fadley and Dr. R. Z. Bachrach for sending us preprints of articles prior to publication.

VI. REFERENCES

* This work was done with support from the U. S. Energy Research and Development Administration and performed in part at the Stanford Synchrotron Radiation Project, which is supported by the NSF Grant No. DMR 73-07692 A02, in cooperation with the Stanford Linear Accelerator Center.

+ Max-Planck Institut für Festkorperforschung, Stuttgart, Federal Republic of Germany.

1. D. E. Eastman in Vacuum Ultraviolet Radiation Physics, ed. E. Koch, R. Haensel, and C. Kunz, (Pergamon, Vieweg, 1974), p. 417.
2. W. E. Spicer in Optical Properties of Solids: New Developments, ed. B. O. Seraphin (North-Holland Publishing Co., Amsterdam 1976) p. 633.
3. D. A. Shirley, Adv. Chem. Phys. 23 (1973) 85.
4. R. E. Watson and M. L. Perlman, Structure and Bonding 24 (1975) 83.
5. P. Feibelman and D. E. Eastman, Phys. Rev. B 10 (1974) 4932.
6. J. B. Pendry, Surface Sci. 57 (1976) 679.
7. C. N. Berglund and W. E. Spicer, Phys. Rev. 136 (1964) A1030.
8. E. Bauer, J. Vac. Sci., Technol. 7 (1969) 3.
9. P. Feibelman, Phys. Rev. B 7 (1973) 2305 and Surface Sci. 36 (1973) 558.
10. S. P. Kowalczyk, L. Ley, F. R. McFeely, R. A. Pollak, and D. A. Shirley, Phys. Rev. B 8 (1973) 3583.
11. M. Šunjić, and D. Šokčević, J. Electron Spectrosc. 5 (1974) 963, and Sol. St. Comm. 18 (1976) 373.

14. G. A. Sawatzky, A. Barrie, and G. Jonkers, private communication.

15. J. C. Fuggle, D. J. Fabian, and L. M. Watson, J. Electron Spectrosc. 9 (1976) 99.

16. R. A. Pollak, Ph.D. thesis, University of California, Lawrence Berkeley Laboratory Report, LBL-1299 (1972) unpublished.

17. H. Weaver, private communication and independently computed by one of us, G. A., using typical lens operating voltages.

18. S. P. Kowalczyk, Ph.D. thesis, University of California, Lawrence Berkeley Laboratory Report, LBL-4319 (1976) unpublished.

19. H. Winick, Ref. 1, p. 776.

20. F. C. Brown, R. Z. Bachrach, S. B. M. Hagstrom, N. Lien, and C. H. Pruett, Ref. 1, p. 785.

21. C. S. Fadley, Ph.D. thesis, University of California, Lawrence Berkeley Laboratory Report, UCRL-19535.

22. L. A. Harris, Surf. Sci. 15 (1969) 77.

23. W. A. Fraser, J. V. Florio, W. N. Delgass, and W. D. Robertson, Surf. Sci. 36 (1973) 661.

24. C. S. Fadley, R. J. Baird, W. Siekhaus, T. Novakov, and S. A. L. Bergström, J. Electron Spectrosc. 4 (1974) 93.

25. C. S. Fadley, Progress in Solid State Chemistry 11 (1976) 265.

26. P. W. Palmberg and T. N. Rhodin, J. App. Phys. 39 (1968) 2425, P. W. Palmberg, Anal. Chem. 45 (1973) 549A.

27. I. Lindau and W. E. Spicer, J. Electron Spectrosc. 3 (1974) 409.

28. C. J. Powell, Surf. Sci. 44 (1974) 29.

29. J. C. Tracy, J. Vac. Sci. Technol. 11 (1974) 280; J. C. Tracy and J. M. Burkstrand, CRC Critical Reviews in Solid State Sciences 4 (1974) 381.

30. G. K. Wertheim and S. Hüfner, J. Inorg. Nucl. Chem 38 (1976) 1701; S. Hüfner, G. K. Wertheim, D. N. E. Buchanan, and K. W. West, Phys. Lett. 46A (1974) 420; S. Hüfner and G. K. Wertheim, Phys. Rev. B. 11 (1975) 678.

31. We wish to point out here that quantitative determinations of photoemission peak broadening must be approached carefully when attempting to relate peak asymmetries to electronic properties of the system studied. Contaminant levels too small to be detected by XPS observation of core lines can be responsible for slight peak broadening (see Fig. 4).

32. C. R. Brundle, Surface Science 48 (1975) 99, and Ref. 26-29.

33. J. E. Houston, R. L. Park and G. E. Laramore, Phys. Rev. Letters 30 (1973) 846.

34. C. Webb and P. M. Williams, Phys. Rev. Letters 33 (1974) 824.

35. J. Stohr, G. Apai, P. S. Wehner, F. R. McFeely, R. S. Williams, and D. A. Shirley, Phys. Rev. B 14 (1976) 5144.

36. D. A. Shirley, R. L. Martin, S. P. Kowalczyk, F. R. McFeeley, and L. Ley, Phys. Rev. B, to be published.

37. H. Raether, Springer Tracts in Modern Physics 38 (1965) 84.

38. R. J. Baird and C. S. Fadley, to appear in the Proceedings of the International Study Conference on Photoemission from Surfaces, Noordwijk, Holland, 1976.

39. D. R. Penn, Phys. Rev. b 13 (1976) 5248.

40. S. A. Flodstrom, R. Z. Bachrach, R. S. Bauer, J. C. McMenamin, and S. B. M. Hagstrom, J. Vac. Sci. Tech. 14 (1977) xxx .

41. L. Kleinman, Phys. Rev. B 3 (1971) 2982.

42. D. R. Penn, J. Electron Spectrosc. 9 (1976) 29.

Table 1

Angular Dependence of Al Plasmons in XPS

Plasmon loss structure	Take-off angle		
	54°	38°	7.5°
Al 2p I_S^O		0.17(1)	
Al 2p I_B^O		0.57(2)	
Al 2s I_S^O	0.11(1)	0.14(1)	0.22(3)
Al 2s I_B^O	0.55(2)	0.58(3)	0.46(6)

FIGURE CAPTIONS

Fig. 1 Experimental geometry for the experiments performed using the storage ring SPEAR as a source of synchrotron radiation is shown. The angle of the sample with the CMA symmetry axis was chosen to maximize the count rate with the angle between the incident photon beam and the CMA symmetry axis fixed. The cross-hatched area illustrates the acceptance cone of the CMA.

Fig. 2 The experimental geometry for the XPS angle resolved experiments is shown, illustrating the concept of effective sampling depth, Λ'_{ee} (Eq. 1). The photon source, monochromatized Al Kα radiation, is fixed with respect to the electron analyzer.

Fig. 3 The XPS spectra of the Al 2s region of an oxidized evaporated film is shown. The oxide peak is greatly enhanced at low take-off angle because of the increased surface sensitivity with smaller effective sampling depth.

Fig. 4 The Al 2s spectral region as a function of take-off angle obtained using Al Kα x-rays. Note that the spectrum taken at $\phi = 7.5^{\circ}$ shows a slight shoulder at higher binding energies due to oxide contamination, even though a scan of the O 1s region revealed no detectable signal.

Fig. 5 This is a representation of the universal curve — the electron attenuation length (Λ_{ee}) as a function of electron kinetic energy. Superimposed on this plot are discrete laboratory photon sources which are commonly used in PES.

Fig. 6 The Al 2p spectral region at various photon energies in the ultra-soft x-ray regime. The in situ evaporated Al film had an oxide component, seen as a shoulder on the Al 2s peak at higher binding energy. The spectra broaden at higher photon energies due to the degradation of the monochromator resolution.

Fig. 7 The Al 2p spectral region obtained with Al Kα ($\hbar\omega \sim 1486$ eV) radiation is shown for a takeoff angle of 38°.

Fig. 8 The In 4d spectral region obtained at various photon energies in the ultra-soft x-ray regime. Note the change in plasmon loss peak intensities between 160 eV and 180 eV.

Fig. 9 The In 4d spectral region obtained with Al Kα radiation.

Fig. 10 This figure shows the predicted dependence for Mg Kα excitation of the first surface and first bulk Al 2p plasmon loss peak intensities normalized to the main peak (I_S^o and I_B^o) on take-off angle and Λ_{sr}, the mean free path for short range inelastic collisions.

Fig. 11 Variation of the surface to bulk plasmon ratios (I_B^o/I_S^o) as a function of electron take-off angle ϕ is shown. The solid line is the predicted ratio variation from Fig. 10 assuming an electron Λ_{ee} of 25 Å. The dashed continuation of the solid curve is proportional to sin ϕ. Experimental values obtained in this study are shown with error bars to denote the uncertainty in the plasmon peak intensity determination.

Fig. 12 Variation of the normalized Al bulk and surface plasmon loss peak intensities (I_B^o and I_S^o) with energy (bottom). The filled circles and the crosses represent I_B^o and I_S^o respectively from this work; the filled diamonds and squares represent the data of Ref. 40. The top portion shows the ratio I_B^o/I_S^o (filled circles from this work, filled squares from Ref. 40).

Fig. 13 The variation of I_B^o (filled circles) and I_S^o (crosses) for plasmon losses following the In 4d peak as a function of photon energy.

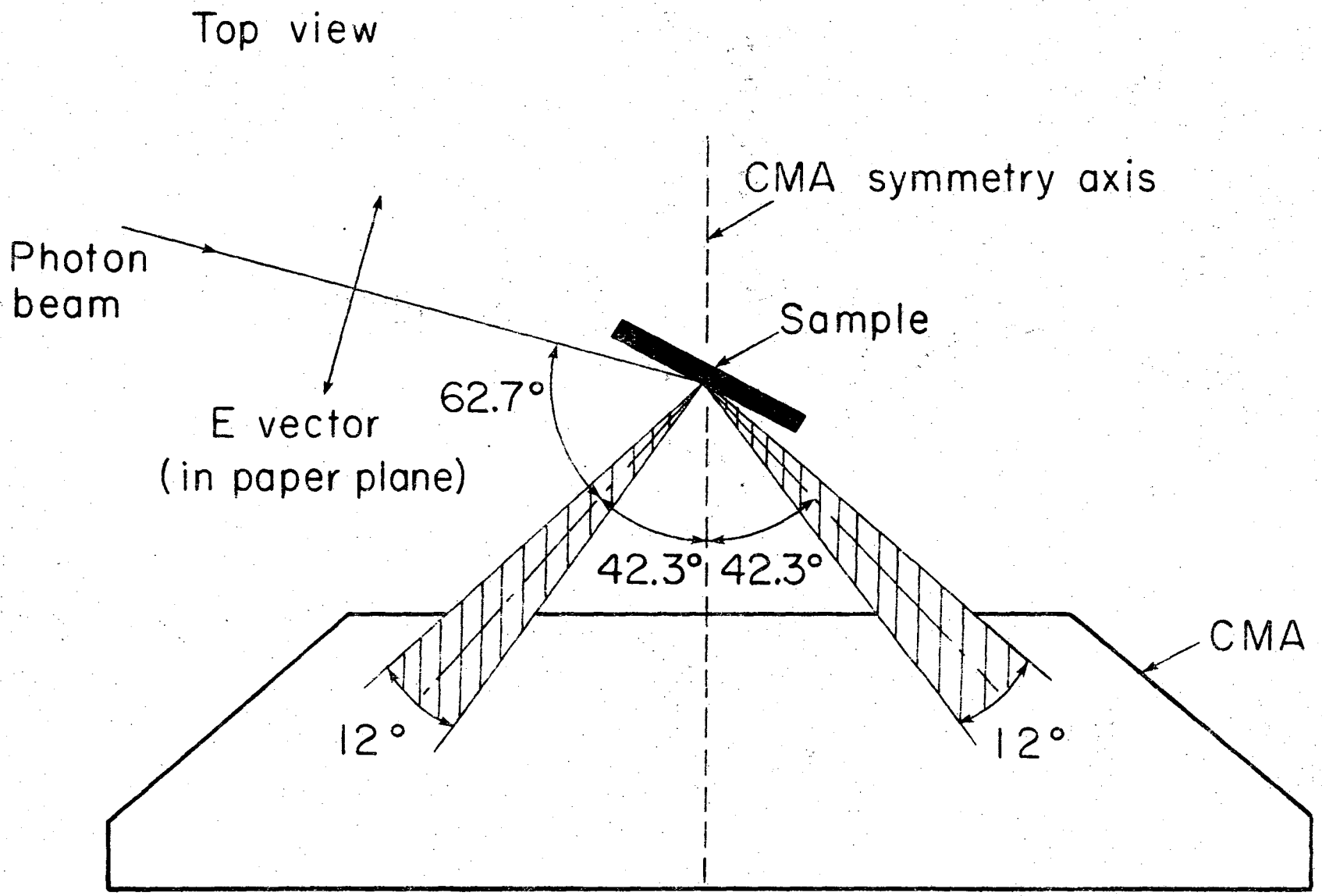

Fig. 1

XBL 764-2732

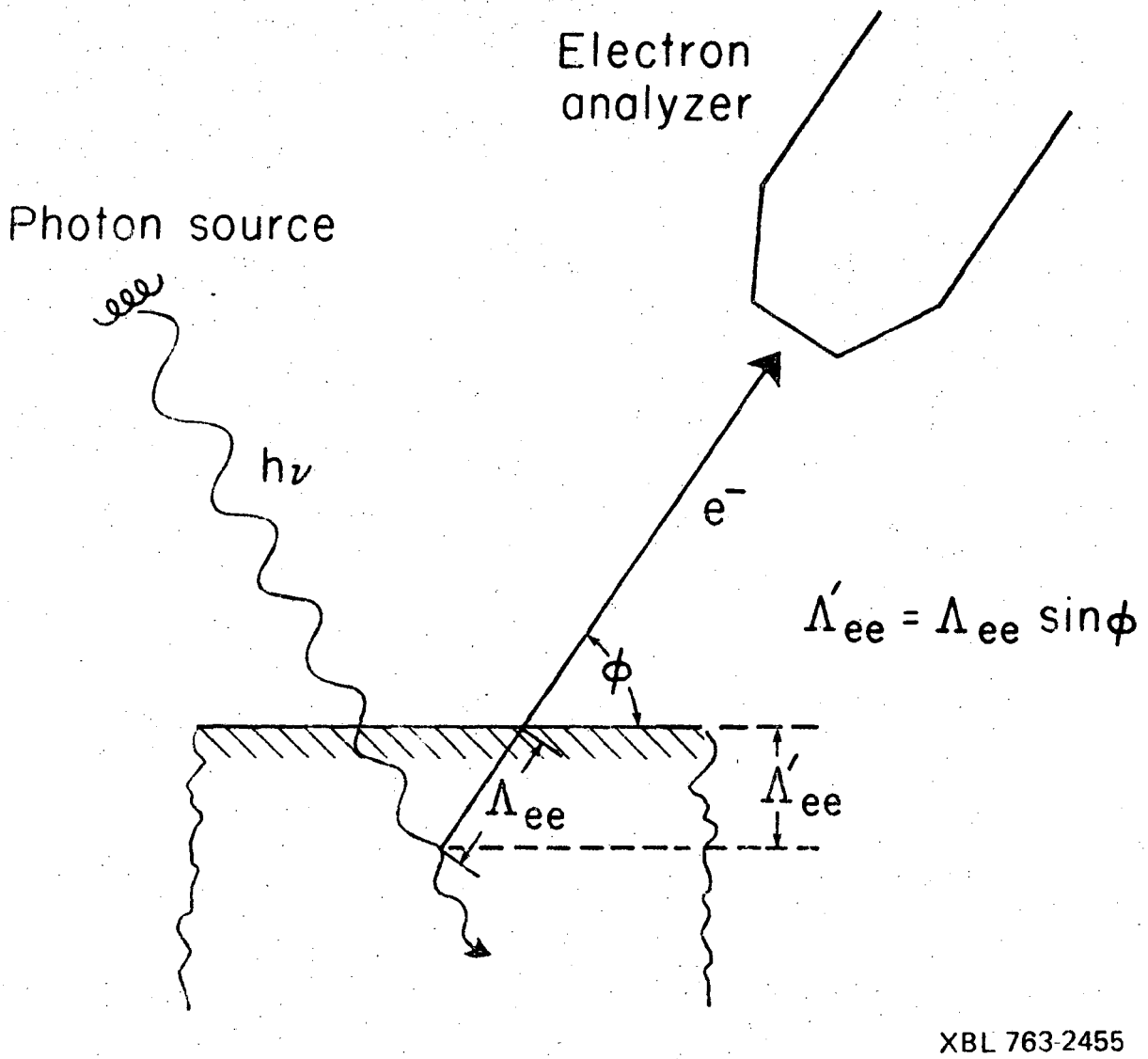
Electron
analyzer
Photon source
hν
e⁻
Λ'ee = Λee sinϕ
ϕ
Λee
Λ'ee
XBL 763-2455

Fig. 2

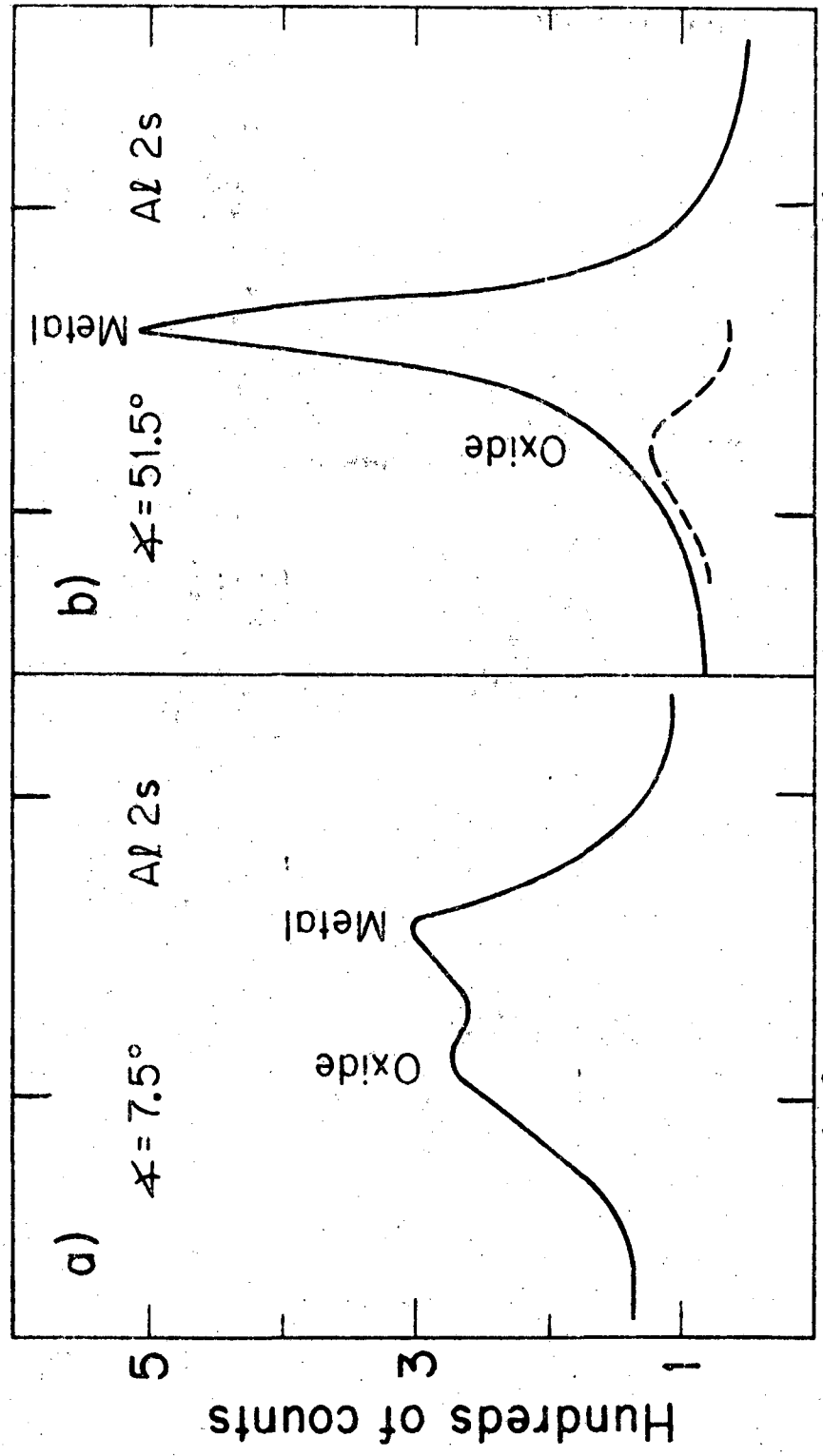

XBL7410-4338

Fig. 3

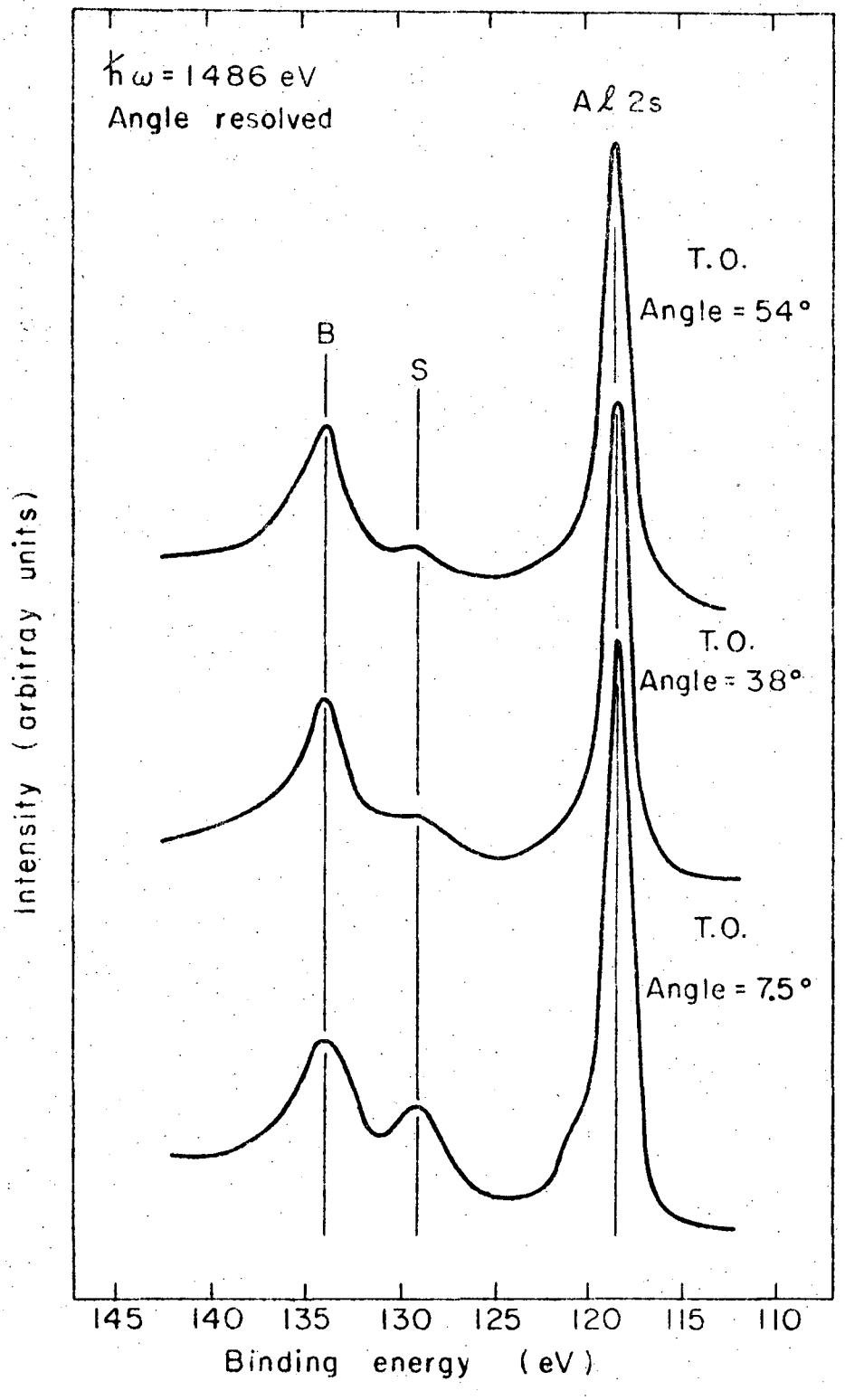

XBL 769-4044

Fig. 4

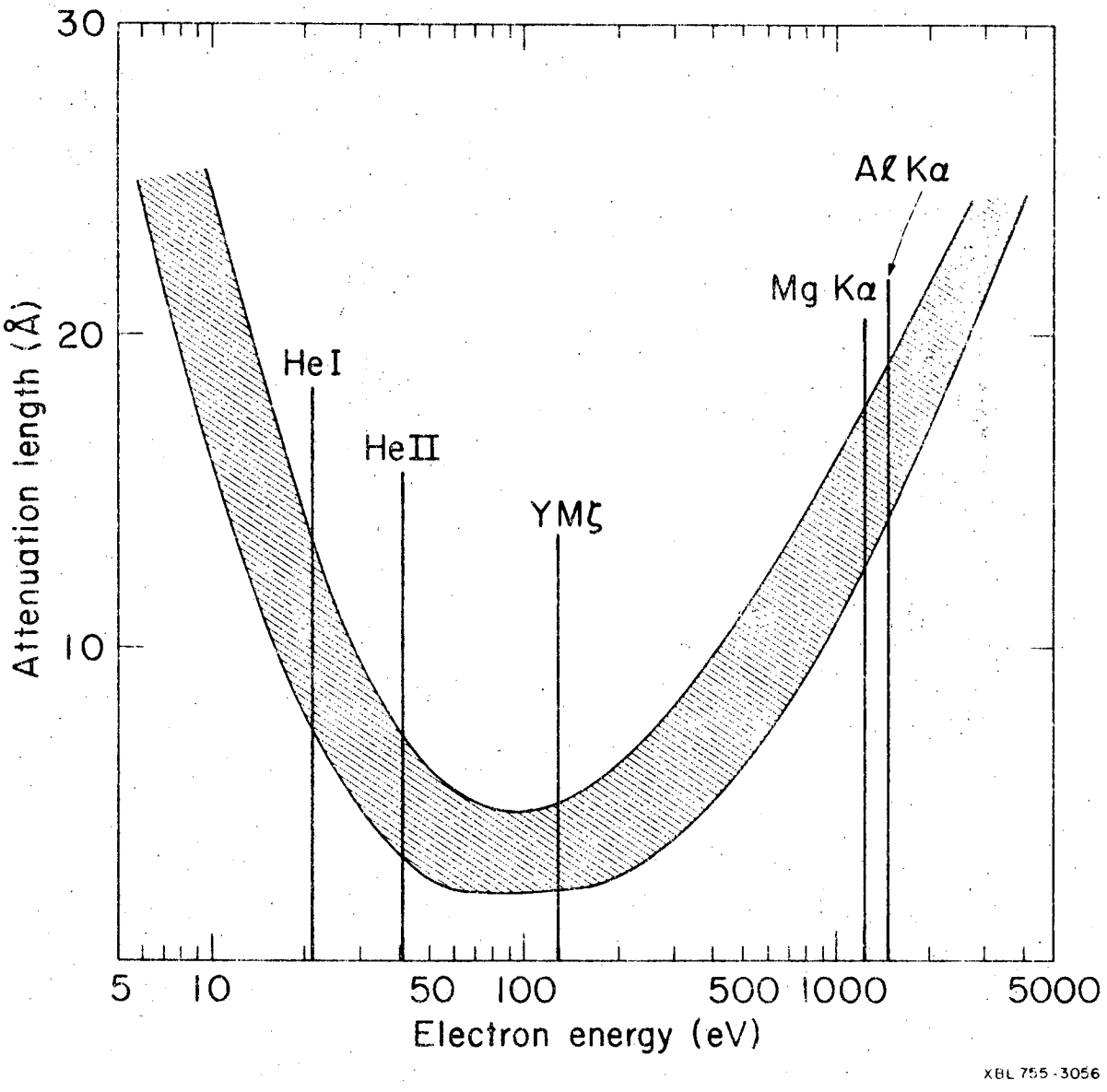

Fig. 5

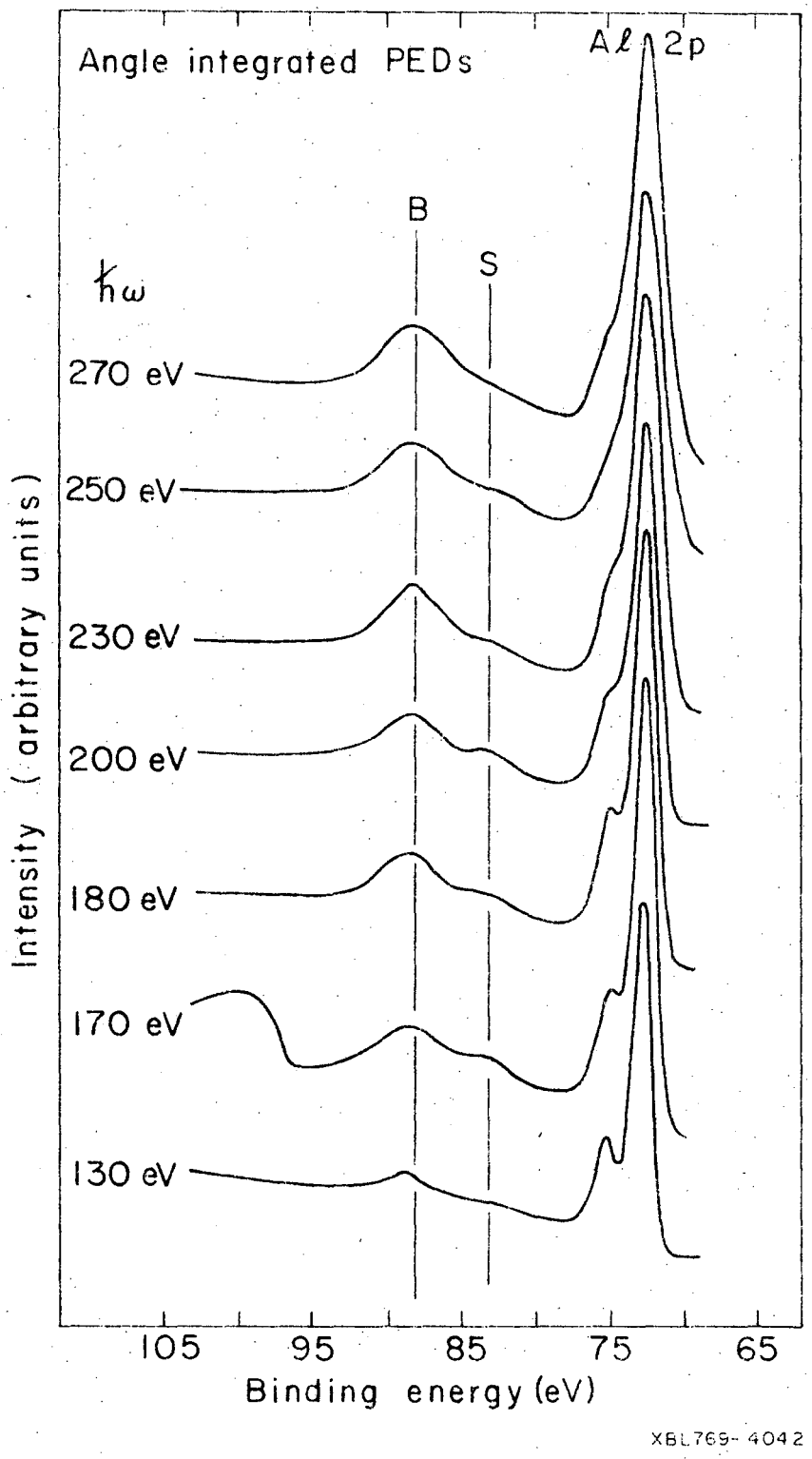
Angle integrated PEDs
Aℓ 2p
B
S
ħω
270 eV
250 eV
230 eV
200 eV
180 eV
170 eV
130 eV
Intensity (arbitrary units)
105
95
85
75
65
Binding energy (eV)
XBL769-4042

Fig. 6

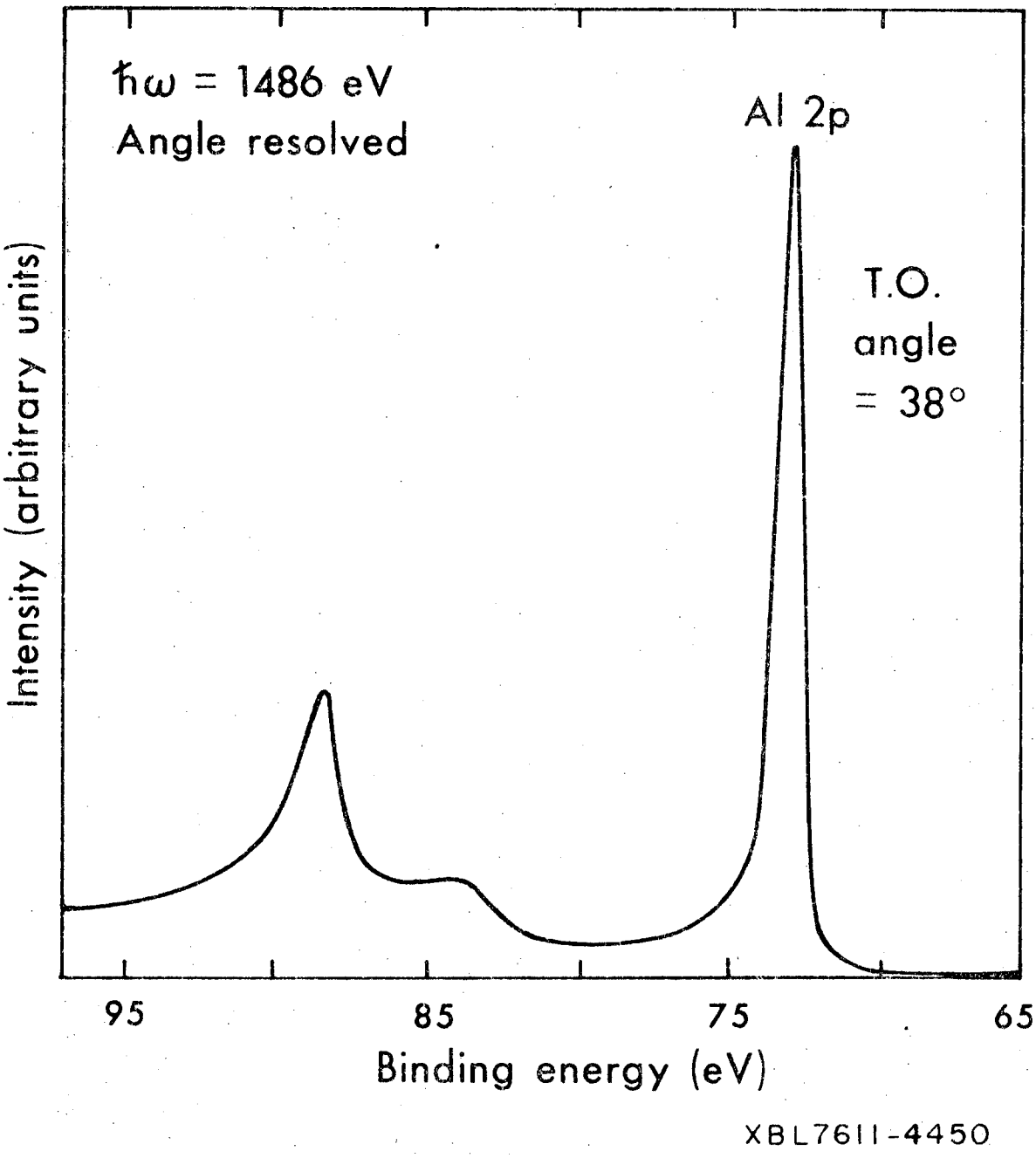

Fig. 7

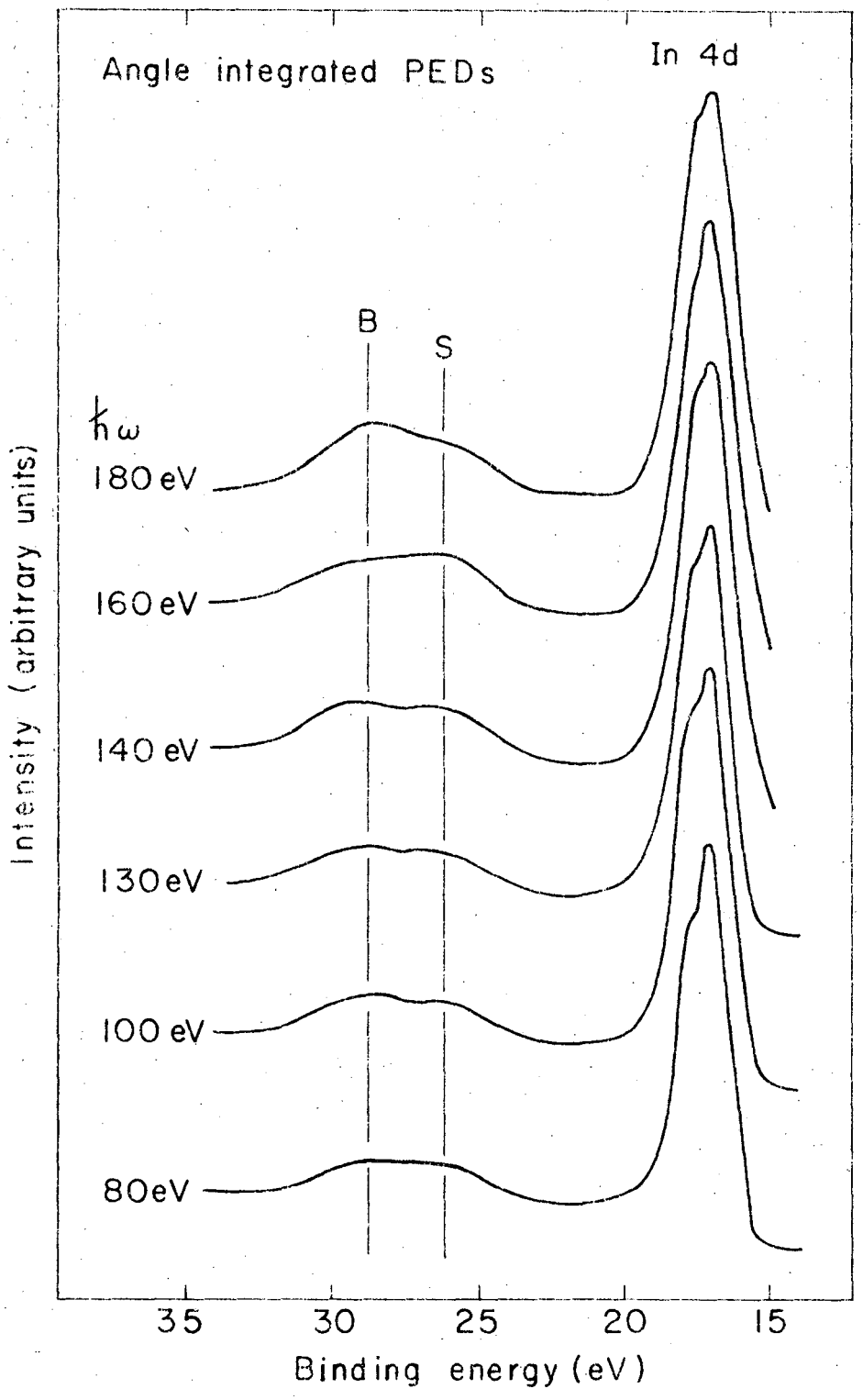

XBL769-4043

Fig. 8

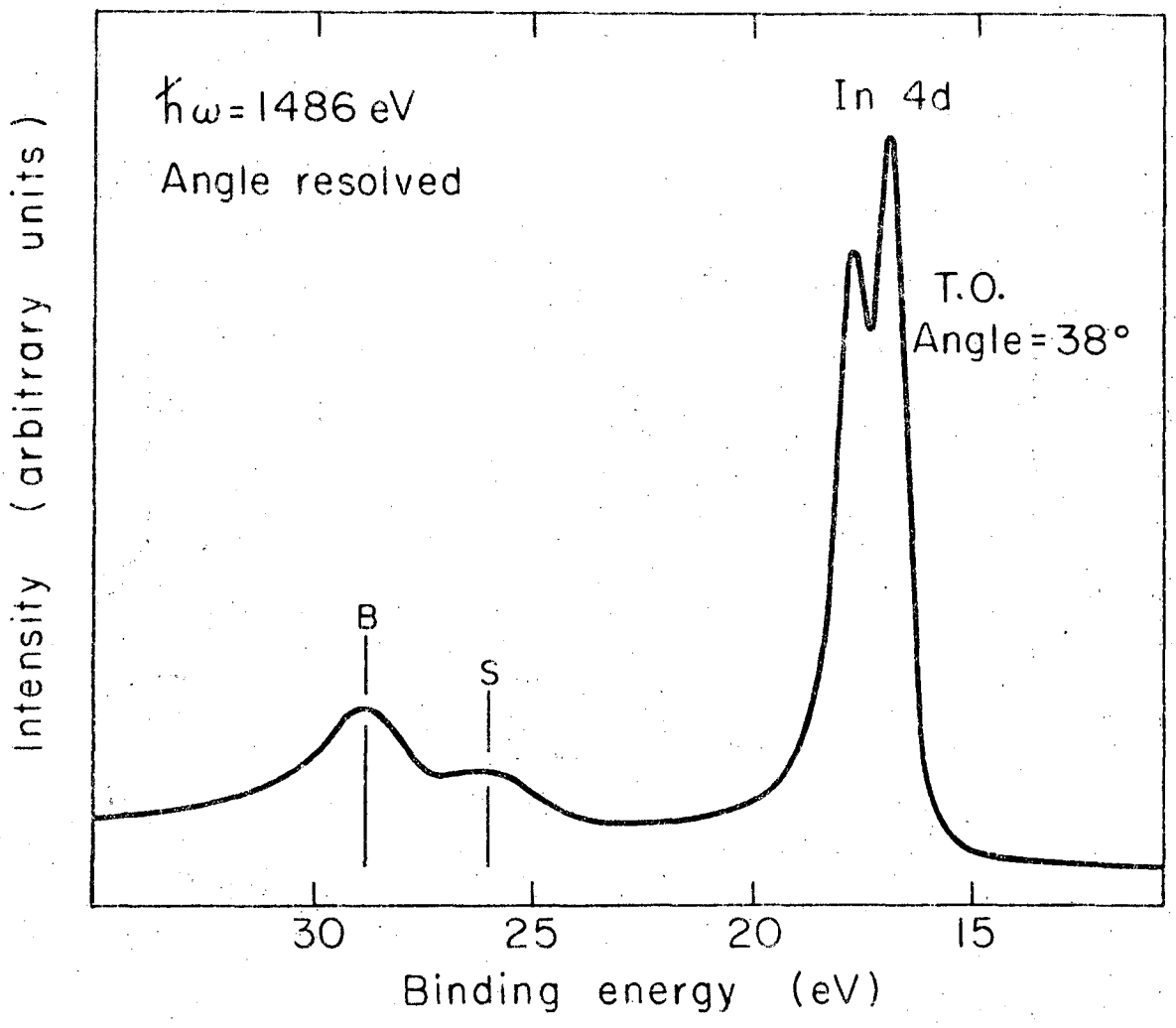

XBL769-4045

Fig. 9

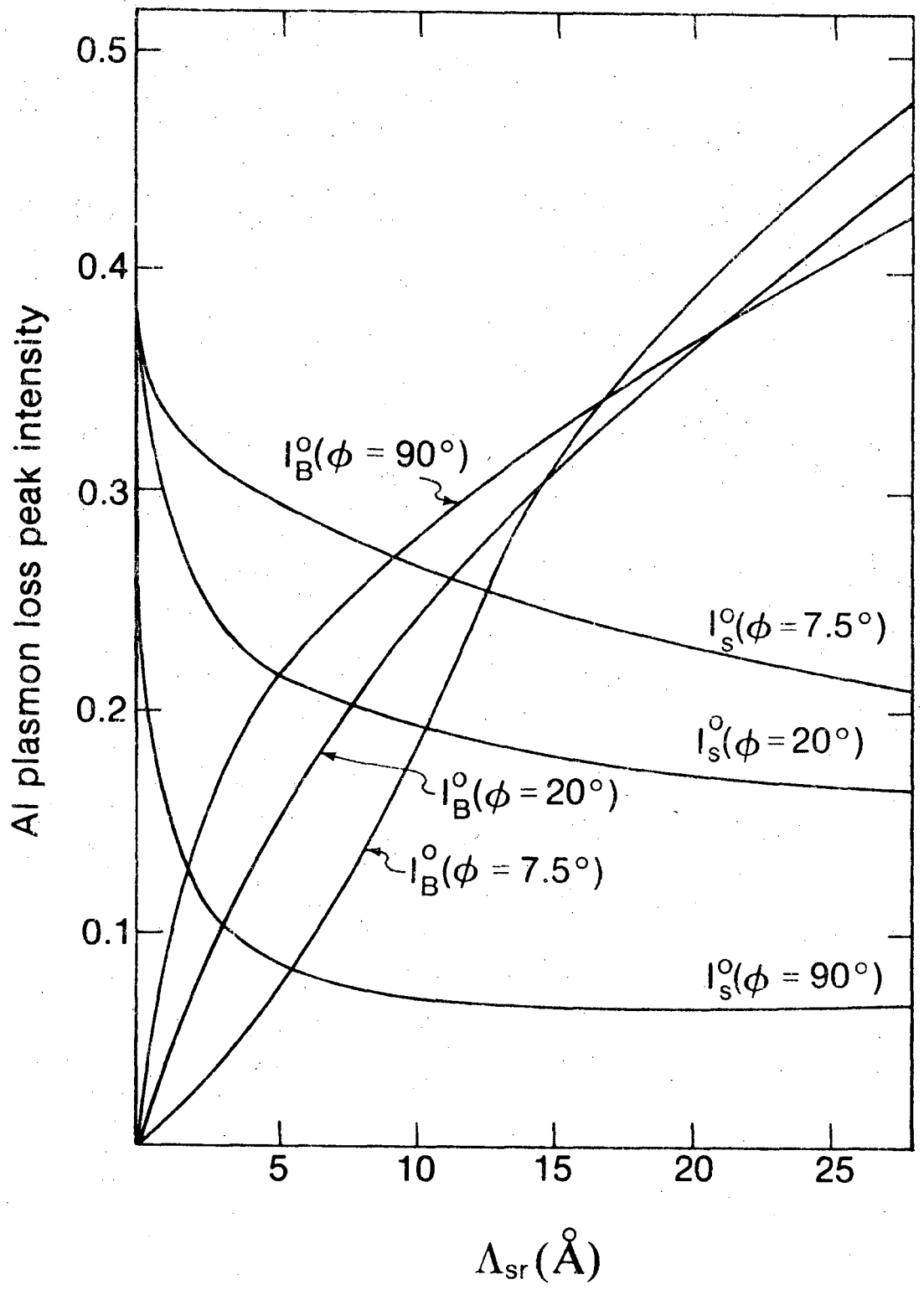

XBL7611-4454

Fig. 10

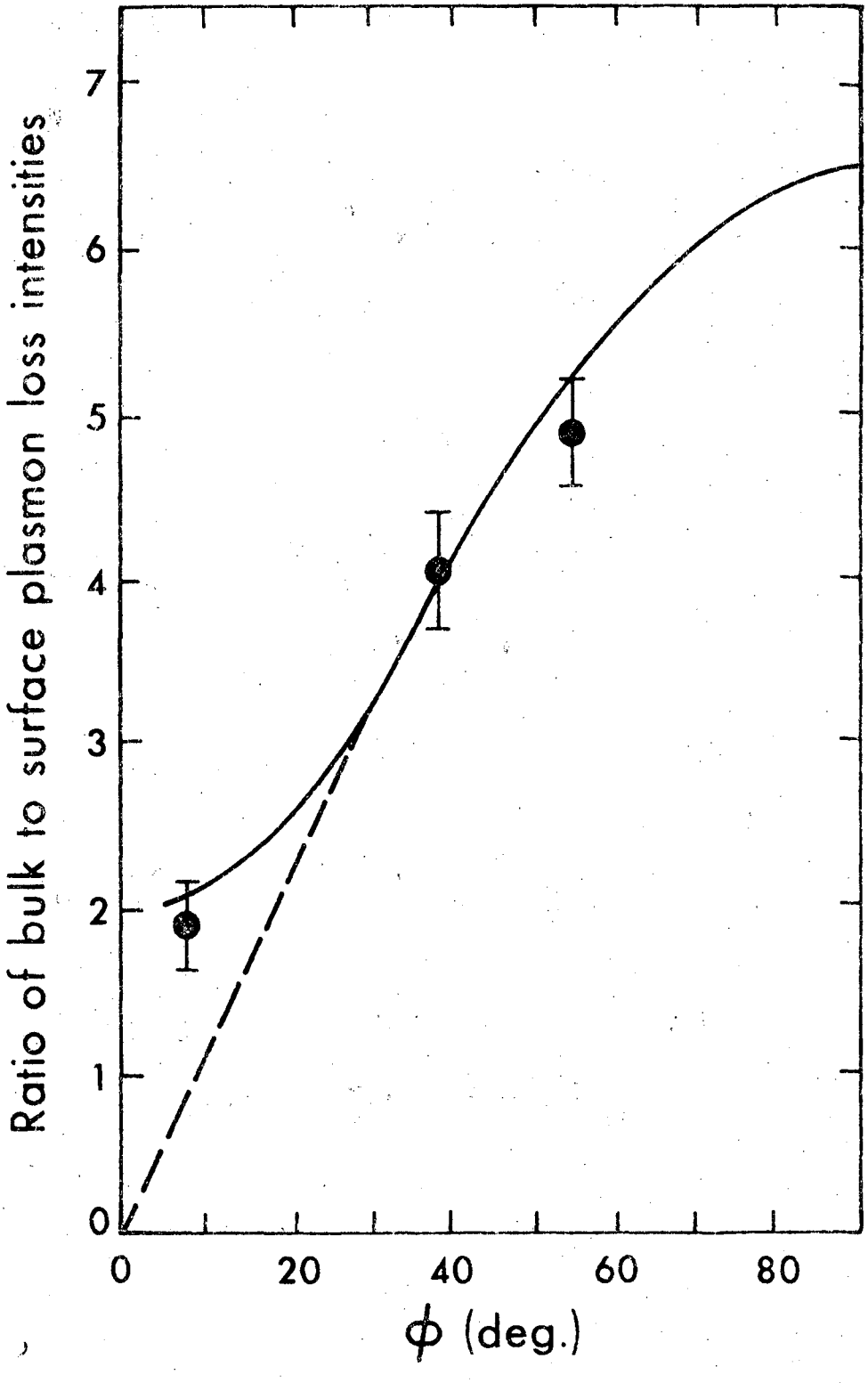

XBL7611-4452

Fig. 11

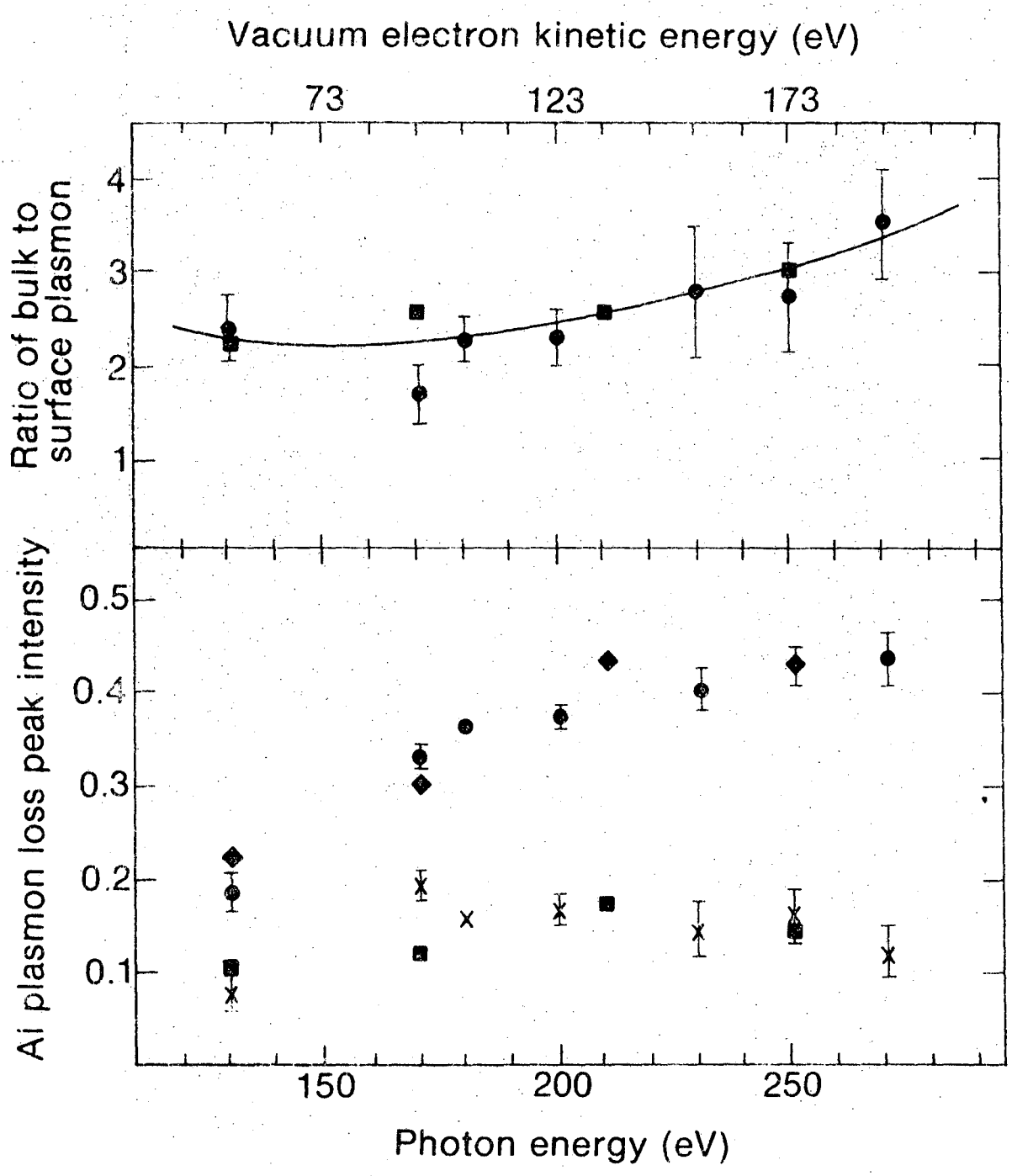

XBL7611-4455

Fig. 12

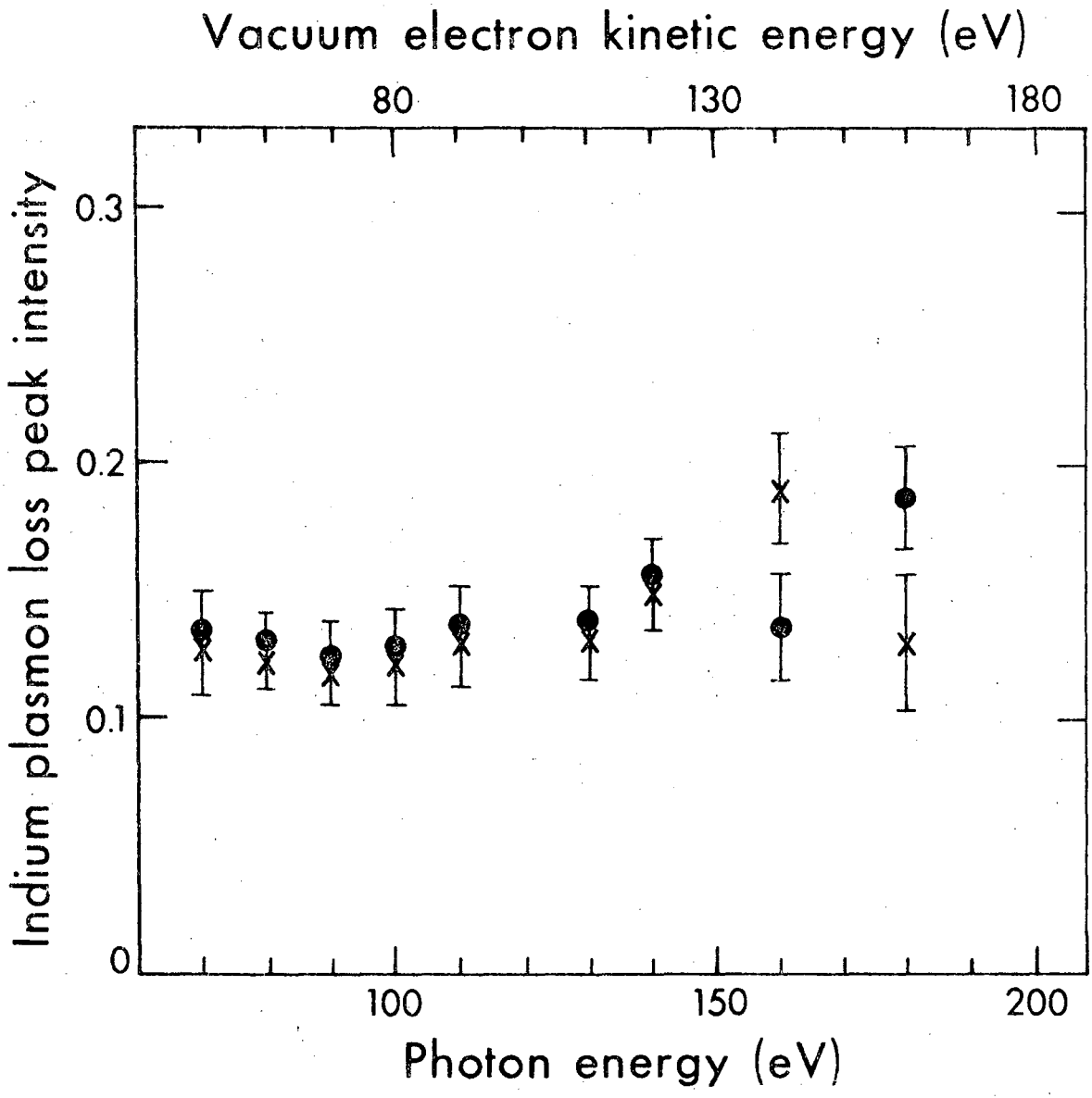

XBL7611-4456

Fig. 13

TECHNICAL INFORMATION DIVISION
LAWRENCE BERKELEY LABORATORY
UNIVERSITY OF CALIFORNIA
BERKELEY, CALIFORNIA 94720